18

Case Study

Composite Bearing—Rolling Elements and Fluid Film in Series

18.1 INTRODUCTION

A composite bearing of rolling and hydrodynamic components in series is a unique design that was proposed initially to overcome two major disadvantages of hydrodynamic journal bearings: Severe wear during start-up and stopping, and risk of catastrophic failure during any interruption of lubricant supply.

18.1.1 Start-Up and Stopping

Hydrodynamic bearings are subjected to severe wear during the starting and stopping of journal rotation. In addition, in variable-speed machines, when a bearing operates at low-speed, there is no full fluid film, resulting in wear. In these cases, there is also a risk of bearing failure due to overheating, which is a major drawback of hydrodynamic journal bearings.

In theory, there is a very thin fluid film even at low journal speeds. But in practice, due to surface roughness, vibrations, and disturbances, a critical minimum speed is required to generate adequate fluid film thickness for complete separation of the sliding surfaces. During start-up, wear is more severe than during stopping, because the bearing accelerates from zero velocity, where there is relatively high static friction. In certain cases, there is stick-slip friction during

bearing start-up (see Harnoy 1966). During start-up, as speed increases, the fluid film builds up and friction reduces gradually.

18.1.2 Interruption of Oil Supply

A hydrodynamic bearing has a high risk of catastrophic failure whenever the lubricant supply is interrupted, even for a short time. The operation of a hydrodynamic journal bearing is completely dependent on a continuous supply of lubricant, particularly at high speed. If the oil supply is interrupted, this can cause overheating and catastrophic (sudden) bearing failure. At high speed, heat is generated at a fast rate by friction. Without lubricant, the bearing can undergo failure in the form of melting of the bearing lining. The lining is often made of a white metal of low melting temperature. Under certain conditions, interruption of the oil supply can result in bearing seizure (the journal and bearing weld together).

Interruption of the oil supply can occur for several reasons, such as a failure of the oil pump or its motor. In addition, the lubricant can be lost due to a leak in the oil system. This risk of failure prevents the use of hydrodynamic bearings in critical applications where safety is a major concern, such as in aircraft engines.

Replacing the hydrodynamic journal bearing with an externally pressurized hydrostatic journal bearing can eliminate the severe wear during starting and stopping. But a hydrostatic journal bearing is uneconomical for many applications because it needs a hydraulic system that includes a pump and an electric motor. For many machines, the use of hydrostatic bearings is not feasible. In addition, an externally pressurized hydrostatic bearing does not eliminate the risk of catastrophic failure in the case of oil supply interruption.

18.1.3 Limitations of Rolling Bearings

Rolling bearings are less sensitive than hydrodynamic bearings to starting and stopping. However, rolling bearing fatigue life is limited, due to alternating rolling contact stresses, particularly at very high speed. This problem is expected to become more important in the future because there is a continuous trend to increase the speed of machines. Manufacturers continually attempt to increase machinery speed in order to reduce the size of machines without reducing power.

It was shown in Chapter 12 that at very high speeds, the centrifugal forces of the rolling elements increase the contact stresses. At high speeds, the temperature of a rolling bearing rises and the fatigue resistance of the material deteriorates. The centrifugal forces and temperature exacerbate the problem and limit the speed of reliable operation. Thus the objective of long rolling bearing life and that of high operating speeds are in conflict. In conclusion, the optimum operation of the rolling bearing occurs at relatively low and medium speeds, while

the best performance of the hydrodynamic bearing happens at relatively high speeds.

Over the years, there has been considerable improvement in rolling bearing materials. By using bearings made of high-purity specialty steels, fatigue life has been extended. High-quality rolling bearings made of specialty steels involve higher cost. These bearings are used in aircraft engines and other unique applications where the high cost is justified. However, since there is a continual requirement for faster speeds, the fatigue life of rolling bearings will continue to be a bottleneck in the future for the development of faster machines.

It would offer considerable advantage if the bearing could operate in a rolling mode at low speed and at higher speed would convert to hydrodynamic fluid film operation. In fact, this is the purpose of the composite bearing that utilizes the desirable features of both the hydrodynamic and the rolling bearing by combining them in series. In addition, if the oil supply is interrupted, the bearing will work in the rolling mode only and thus eliminate the high risk of failure of the common fluid film bearing.

In the following discussion, it is shown that it is possible to mitigate the drawbacks of the hydrodynamic journal bearing by using a *composite bearing*, which is a unique design of hydrodynamic and rolling bearings in series. In previous publications, this design was also referred to as the *series hybrid bearing*, the *angular-compliant bearing* and *hydro-roll*.

18.2 COMPOSITE-BEARING DESIGNS

The combination was tested initially (Harnoy 1966; Lowey, Harnoy, and Bar-Nefi 1972) by inserting the journal directly in the rolling-element inner ring bore; see Fig. 18-1. They used a radial clearance commonly accepted in hydrodynamic journal bearings of the order of magnitude $C \approx 10^{-3} \times R$. Later, this combination was improved (see Harnoy 1966), by inserting a sleeve at a tight fit into the bore of the rolling bearing; see Fig. 18-2. The journal runs on a fluid film in a free-fit clearance inside the bore of this sleeve. In this way, the desired sleeve material and surface finish can be selected as well as the ratio of the length and diameter, L/D, of the sleeve. In many applications, a self-aligning rolling element is desirable to ensure parallelism of the fluid film surfaces. The lubrication is an oil bath arrangement. The oil is fed in the axial direction of the clearance to form a fluid film between the journal and the sleeve; see Fig. 18-2.

Anderson* (1973) suggested a practical combination for use in gas turbines; see Fig. 18-3. This is a combination of a conical hydrodynamic bearing

* It is interesting that the work by the NASA group headed by Anderson and that of Lowey, Harnoy and Bar-Nefi in the Technion–Israel Institute of Technology were performed independently, without any knowledge of each other's work.

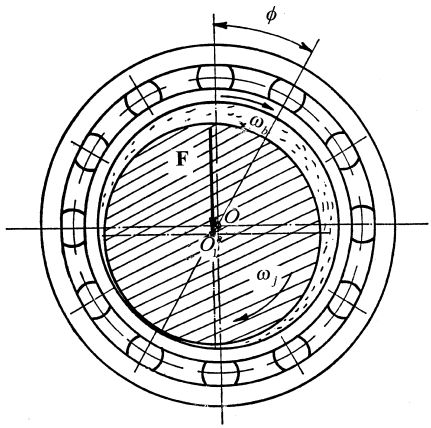

FIG. 18-1 Composite bearing arrangement of hydrodynamic and rolling bearings in series. (From Harnoy, 1966.)

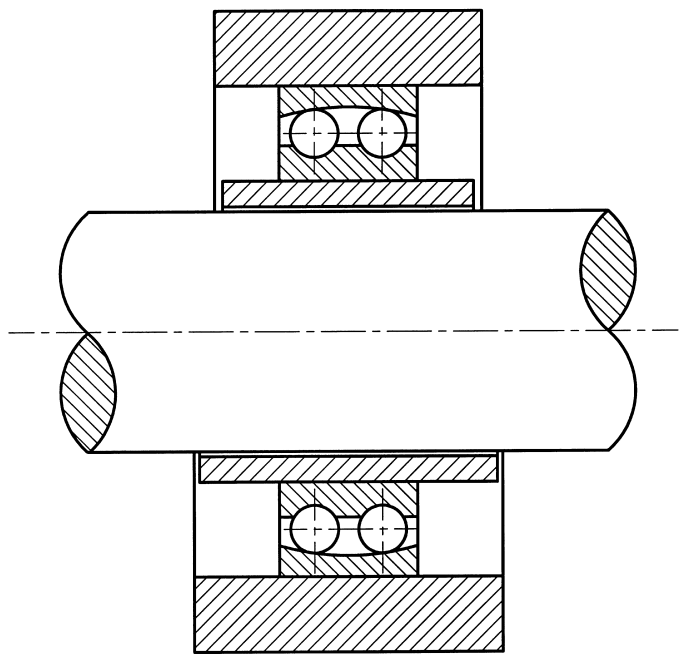

FIG. 18-2 Composite-bearing design with inner sleeve. (From Harnoy, 1966.)

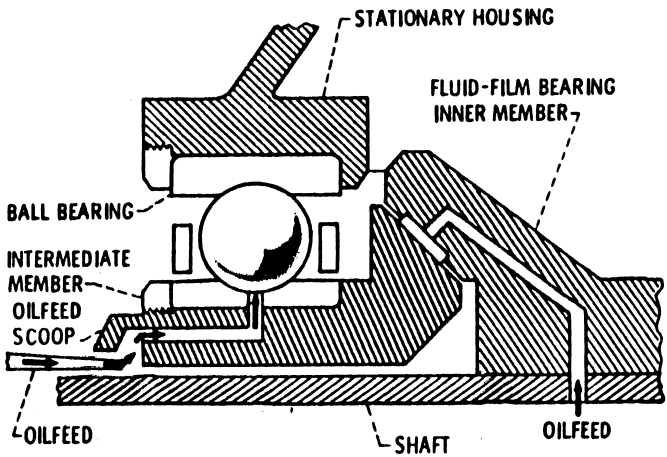

FIG. 18-3 Anderson composite bearing for radial and thrust loads. (From Anderson, 1973.)

and a rolling bearing in series, to provide for thrust and radial loads in gas turbine engines.

In the foregoing combinations of hydrodynamic and rolling bearings in series, the rolling-element bearing operates in rolling mode at low speed, including starting and stopping, while a sliding mode of the hydrodynamic fluid film is initiated at higher speed. The benefits of this combination are reduction of friction and wear and longer bearing life due to reduction of rolling speed.

It was mentioned earlier that the risk of catastrophic failure is the reason that hydrodynamic bearings are not applied in critical applications where safety is involved, such as aircraft engines. In fact, the composite bearing can overcome this problem, because, in the case of oil supply interruption, the composite bearing would continue to operate in the rolling mode, which requires only a very small amount of lubricant.

It is interesting to note that there are also considerable advantages in a hybrid bearing in which the rolling and hydrodynamic bearings are combined in parallel. Wilcock and Winn (1973) suggested the parallel combination.

18.2.1 Friction Characteristics of the Composite Bearing

In Fig. 18-4, f–U curves (friction coefficient versus velocity) are shown of a rolling bearing and of a fluid film bearing. These are the well-known Stribeck curves. Discussion of the various regions of the fluid film friction curve is included

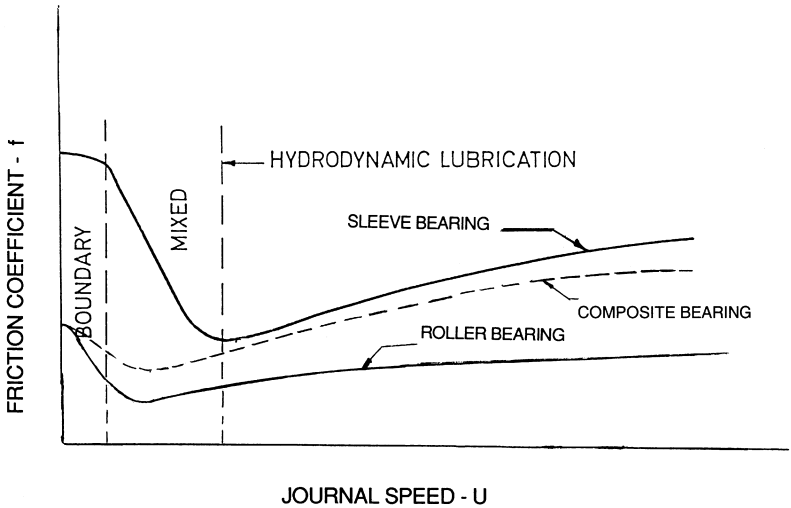

FIG. 18-4 Friction coefficient as a function of speed. (From Harnoy and Khonsari, 1996.)

in Chapter 8; measurement methods are covered in Chapter 14. The following discussion shows that the composite bearing, in fact, improves the friction characteristics by eliminating the high start-up friction of a fluid-film bearing.

The sleeve bearing friction curve in Fig. 18-4 has high friction in the boundary and mixed lubrication regions because the sliding surface asperities are in direct contact at low speed. In the hydrodynamic lubrication region, the sliding surfaces are separated by a fluid film and viscous friction is increasing almost linearly with speed. The curve for rolling bearing friction is similar, but start-up friction and high-speed friction are much lower than that of the common sleeve bearing.

The purpose of the composite bearing is to avoid the high friction in the boundary lubrication region and most of the mixed region of a sleeve bearing. In Fig. 18-4, the dotted line shows the expected friction characteristic of a properly designed composite bearing. During start-up, the composite bearing operates as a rolling bearing and the starting friction is as low as in a rolling bearing. The friction coefficient at the high rated speed is expected to be somewhat lower than for a regular journal bearing. This is because the viscous friction is proportional to the sliding speed only and the total speed of a composite bearing is divided into rolling and sliding parts.

18.2.2 Composite-Bearing Start-Up

During start-up, the sliding friction of a hydrodynamic bearing is higher than that of a rolling bearing. Therefore, sliding between the journal and the sleeve is

replaced by a rolling action (similar to that in an internal gear mechanism). Thus the surface velocity of the shaft, $R\omega_j$, is equal to the velocity of the sleeve bore surface, $R_1\omega_b$. The velocities are shown in Fig. 18-1. The difference between the journal and bore surface radii is small and negligible, so we can assume $R_1 = R$.

An important aspect in the operation of a composite bearing is that the friction during the transition from rolling to sliding is significantly lower than for a regular start-up of a regular hydrodynamic journal bearing. The friction is lower because the initial rolling generates a fluid film between the rolling surfaces of the journal and the sleeve bore. This effect is explained next according to hydrodynamic theory.

18.2.3 Analysis of Start-up

For bearings under steady conditions, if the bearing sleeve and the journal are rotating at different speeds, the Reynolds equation for incompressible and isothermal conditions reduces to the following form [see Eq. (6-21b)]:

$$\frac{\partial}{\partial x}\left(\frac{h^3}{\mu}\frac{\partial p}{\partial x}\right) + \frac{\partial}{\partial z}\left(\frac{h^3}{\mu}\frac{\partial p}{\partial z}\right) = 6R(\omega_j + \omega_b)\frac{\partial h}{\partial x} \tag{18-1}$$

The surface velocities of bearing and journal, $R\omega_j$ and $R_1\omega_b$, respectively, are shown in Fig. 18-1. In Eq. (18-1), p is the pressure and h is the fluid film thickness. For a regular journal bearing, there is only journal rotation, i.e., one surface has velocity $R\omega_j$ while the sleeve is stationary. After integration of Eq. (18-1), the pressure distribution in the fluid film and the load capacity are directly proportional to the sum $R(\omega_j + \omega_b)$.

During start-up, there is only the rolling mode, and the boundary conditions of the fluid film are

$$R\omega_j = R_1\omega_b \tag{18-2}$$

In comparison, in a regular journal bearing of a stationary sleeve, $\omega_b = 0$. Therefore, in the case of pure rolling, the sum of the velocities is double that of pure sliding in a common journal bearing. This means that during start-up, the fluid film pressure of a composite bearing is double that in a common hydrodynamic journal bearing, where $\omega_b = 0$. In the rolling mode, only half of the journal speed is required to generate the film thickness of a regular bearing with a stationary sleeve. This film of the rolling mode prevents wear and high friction at the transition from rolling to sliding.

The physical explanation is that the fluid is squeezed faster by the rolling action than by sliding. Doubling the pressure via rolling action is well known for those involved in the analysis of EHD lubrication of rolling elements.

18.3 PREVIOUS RESEARCH IN COMPOSITE BEARINGS

Experiments by Harnoy (1966) demonstrated that the composite bearing operates as a rolling element during starting and stopping, while hydrodynamic sliding is initiated at higher speeds. At the high rated speed, the rolling element rotates at a reduced speed because the speed is divided between rolling and sliding modes according to a certain ratio. The reduction of the rolling-element speed offers the important advantage of extending rolling bearing life. The composite bearing has a longer life than either a rolling bearing or fluid film bearing on its own. In addition, if the oil supply is interrupted, the composite bearing converts to rolling bearing mode, and the risk of a catastrophic failure is eliminated.

Developments in aircraft turbines generated a continual need for bearings that can operate at very high speeds. As discussed earlier, only rolling bearings are used in aircraft engines, because of the risk of oil supply interruptions in fluid film bearings. The centrifugal forces of the rolling elements is a major bottleneck limiting the speed of aircraft gas turbines.

The centrifugal forces dramatically increase with the DN value (the product of rolling bearing bore in millimeters and shaft speed in revolutions per minute). The centrifugal force of the rolling elements is a reason for limiting aircraft turbine engines to 2 million DN. This was NASA's motivation for initiating a research program to find a better bearing design for high-speed applications. Several ideas were tested to break through the limit of 2 million DN. Ball bearings with hollow balls were tested to reduce the mass of the rolling elements. Later, the introduction of silicone nitride rolling elements proved to be more effective in this direction (see Chapter 13).

In the early 1970s, a research team at the NASA Lewis Research Center did a lot of research and development work on the performance of the composite bearing (for example, Anderson, Fleming, and Parker 1972, and Scribbe, Winn, and Eusepi 1976). The NASA team refers to the composite bearing as a *series hybrid bearing*. The objective was to reach a speed of 3 million DN. The idea was to reduce the rolling-element speed by introducing a fluid film bearing in series that would participate in a portion of the total speed of the shaft. In fact, this work was successful, and operation at 3 million DN was demonstrated. This work proved that the composite bearing is a feasible alternative to conventional rolling bearings in aircraft turbines. Ratios of rolling-element speed to shaft speed (ω_b/ω_j) of a series hybrid bearing were tested by Anderson, Fleming, and Parker (1972). The results, a function of the shaft speed, are shown for two thrust loads in Fig. 18-5.

However, the composite bearing never reached the stage of actual application in aircraft engines, because better rolling-element bearings were developed that satisfied the maximum-speed requirement. In addition, the actual speed of aircraft engines did not reach the high DN values that had been expected earlier.

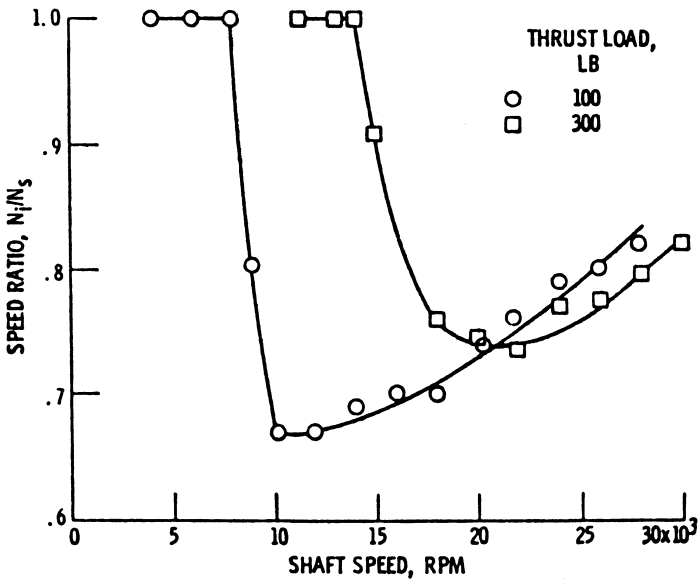

FIG. 18-5 Ratio of inner race speed to shaft speed vs. shaft speed for the composite bearing. (From Anderson, Fleming, and Parker, 1972.)

However, the requirement for higher speeds is increasing all the time. In the future, should the speed requirement increase above the limits of conventional rolling bearings, the composite bearing can offer a ready solution. Moreover, the composite bearing can significantly reduce the high cost of aircraft maintenance that involves frequent-replacement of rolling bearings.* Although the composite bearing has not yet been used in actual aircraft, it can be expected that this low-cost design will find many other applications in the future. The advantages of the composite bearing justify its use in a variety of applications as a viable low-cost alternative to the hydrostatic bearing.

18.4 COMPOSITE BEARING WITH CENTRIFUGAL MECHANISM

The composite arrangement always reduced the rolling element's speed. However, the results are not always completely satisfactory, because the rolling speed is not low enough. Experiments have indicated that in many cases the rolling speed in the composite bearing in Fig. 18-2 is too high for a significant improvement in

* The U.S. Air Force spends over $20 million annually on replacing rolling-element bearings (Valenti, 1995).

fatigue life. Whenever the friction of the rolling-element bearing is much lower than that of the hydrodynamic journal bearing, the rolling element rotates at relatively high speed. To improve this combination, a few ideas were suggested to control the composite bearing and to restrict the rotation of the rolling elements to a desired speed.

In Fig. 18-6a, a design is shown where the sleeve is connected to a mechanism similar to a centrifugal clutch; see Harnoy and Rachoor (1993). A design based on a similar principle was suggested by Silver (1972). A disc with radial holes is tightly fitted on the sleeve and pins slide along radial holes. Due to the action of centrifugal force, a friction torque is generated between the pins and the housing that increases with sleeve speed. This friction torque restricts the rolling speed and determines the speed of transition from rolling to sliding. The centrifugal design allows the sleeve to rotate continuously at low speed. This offers additional advantages, such as enhanced heat transfer from the lubrication film, (Harnoy and Khonsari, 1996) and improved performance under dynamic conditions, (Harnoy and Rachoor, 1993). Long life of the rolling element is maintained because the rolling speed is low. This design has considerable advantages, in particular for high-speed machinery that involves frequent start-ups. Figure 18-6b is a design of a composite bearing for radial and thrust loads with adjustable arrangement.

It is possible to increase the speeds $(\omega_b + \omega_j)$ during the transition from rolling to sliding, resulting in a thicker fluid film at that instant. This can be achieved by means of a unique design of a delayed centrifugal mechanism where the motion of the pins is damped as shown in Fig. 18-7. The purpose of this mechanism is to delay the transition from rolling to sliding during start-up, resulting in higher speeds $(\omega_b + \omega_j)$ at the instant of transition. The delayed action is advantageous only during the start-up, when the wear is more severe than that during the stopping period, since a certain time is required to form a lubricant film or to squeeze it out.

18.4.1 Design for the Desired Rolling Speed

The following derivation is required for the design of a centrifugal mechanism with the desired rolling speed, ω_b. The derivation is for a short journal bearing and a typical ball bearing.

The steady rolling speed ω_b can be solved from the friction torque balance, acting on the sleeve system—a combination of the sleeve and the centrifugal mechanism. The hydrodynamic torque, M_h, of a short bearing is:

$$M_h = \frac{L\mu R^3}{C}(\omega_j - \omega_b)\frac{2\pi}{(1-\varepsilon^2)^{0.5}} \tag{18-3}$$

Here, $R(\omega_j - \omega_b)$ replaces U in Eq. (7-29).

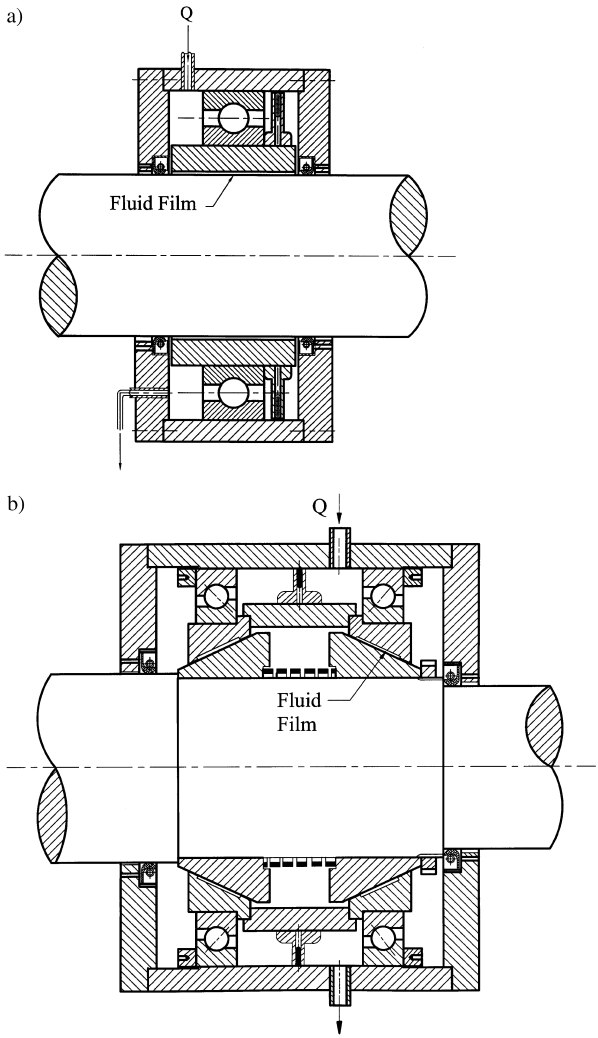

FIG. 18-6 (a) Centrifugal mechanism to control rolling speeds. (b) Composite bearing with centrifugal restraint for radial and thrust loads.

The mechanical friction torque on the sleeve is due to the centrifugal force of the pins, F_c, and the friction coefficient, f_c, between the pins and the housing at radius R_h; see Fig. 18-7:

$$M_f = F_c R_h f_c \tag{18-4}$$

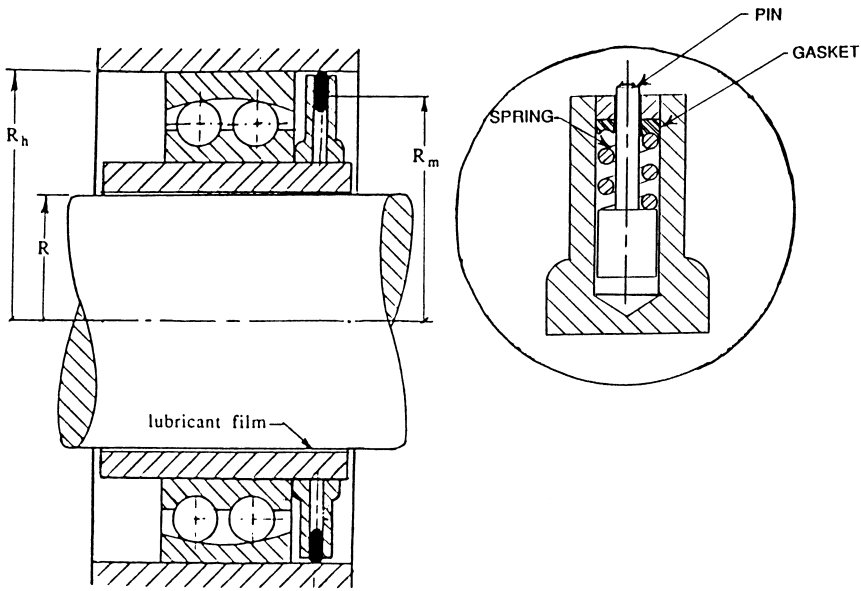

FIG. 18-7 Composite bearing with delayed centrifugal constraint.

The centrifugal contact force, F_c, between the small pins of total mass m_c and the housing is

$$F_c = m_c R_m \omega_b^2 \tag{18-5}$$

Here, m_c is the total mass of the centrifugal pins and R_m is the radius of the circle of the center of the pins when they are in contact with the housing. After substitution of this F_c in Eq. (18-4), the equation of the friction torque becomes

$$M_f = m_c R_m R_h \omega_b^2 f_c \tag{18-6}$$

The contact area between the pins and the housing is small, so boundary lubrication can be expected at all speeds. Thus, the friction coefficient f_c is effectively constant.

The friction torque due to centrifugal action of the pins, M_f, acts in the direction opposite to the hydrodynamic torque. If the composite bearing operates under steady conditions, there is no inertial torque and the equilibrium equation is

$$\frac{2\pi L \mu R^3}{C} \frac{\omega_j - \omega_b}{(1-\varepsilon^2)^{0.5}} = f_c m_c R_m R_h \omega_b^2 + M_r \tag{18-7}$$

The friction torque M_r of a ball bearing at low speeds is generally much lower than the hydrodynamic friction torque at high speeds, so M_r can be neglected in

Eq. (18-7); see Fig. 18-4. However, in certain cases, such as in a tightly fitted conical bearing, the rolling friction is significant and should be considered. Equation (18-7) yields the following solution for the rolling speed ω_b:

$$\omega_b = \frac{(n^2 + mq)^{0.5} - n}{m} \tag{18-8}$$

where

$$m = f_c m_c R_m R_h \tag{18-9}$$

$$n = \pi L \mu R^3 C (1 - \varepsilon^2)^{0.5} \tag{18-10}$$

$$q = 2n\omega_j \tag{18-11}$$

The speed ω_b can be determined by selecting the mass of the pins m_c.

18.5 PERFORMANCE UNDER DYNAMIC CONDITIONS

The advantages of the composite bearing are quite obvious under steady constant load. However, the composite bearing did not gain wide acceptance, because there were concerns about possible adverse effects under unsteady or oscillating loads (dynamic loads). In rotating machinery, there are always vibrations and the average load is superimposed by oscillating forces at various frequencies. Harnoy and Rachoor (1993) analyzed the response of a composite bearing with a centrifugal mechanism, as shown in Fig. 18-6a and b, under dynamic conditions of a steady load superimposed with an oscillating load. The analysis involves angular oscillations of the sleeve, time-variable eccentricity, and unsteady fluid film pressure.

This analysis is essential for predicting any possible adverse effects of the composite arrangement on the bearing stability. Most probably, the unstable region is not identical to that of the common fluid film bearing. Nevertheless, there are reasons to expect improved performance within the stable region.

The following is an explanation of the criteria for improved bearing performance under dynamic loads and why composite bearings are expected to contribute to such an improvement. Unlike operation under steady conditions, where the journal center is stationary, under dynamic conditions, such as sinusoidal force, the journal center, O_1 is in continuous motion (trajectory) relative to the sleeve center O, and the eccentricity e varies with time. For a periodic load, such as in engines, the journal center O_1 reaches a steady-state trajectory referred to as *journal locus* that repeats in each time period. If the maximum eccentricity e_m of this locus (the maximum distance O–O_1 in Fig. 18-1) were to be reduced by the composite arrangement in comparison to the

common journal bearing, it would mean that there is an important improvement in bearing performance. When the eccentricity ratio $\varepsilon = e/C$ approaches 1, there is contact and wear of the journal and sleeve surfaces. As discussed in previous chapters, due to surface roughness, dust, and disturbances, ε_m must be kept low (relative to 1) to prevent bearing wear.

Of course, one can reduce the maximum eccentricity of the locus by simply increasing the oil viscosity, μ; however, this is undesirable because it will increase the viscous friction. If it can be shown that a composite bearing can reduce the maximum eccentricity e_m, for the same viscosity and dynamic loads, then there is a potential for energy savings. In that case, it would be possible to reduce the viscosity and viscous losses without increasing the wear.

There is a simple physical explanation for expecting a significant improvement in the performance of a composite bearing under dynamic conditions, namely, the relative reduction of e_m under oscillating loads. Let us consider a bearing under sinusoidal load. During the cycle period, the critical time is when the load approaches its peak value. At that instant, the journal center, O_1 is moving in the radial direction (away from the bearing center O) and the eccentricity e approaches its maximum value e_m. At that instant, the fluid film is squeezed to its minimum thickness.

Under dynamic load, a significant part of the load capacity of the fluid film is proportional to the sum of the journal and sleeve rotations $(\omega_b + \omega_j)$ [see Eq. (18-1)]. As the external force increases, the fluid film is squeezed and the hydrodynamic friction torque, M_h, increases as well, causing the sleeve to rotate faster (ω_b increases). At that critical instant, the fluid film load capacity increases, due to a rise in $(\omega_b + \omega_j)$, in the direction directly opposing the journal motion toward the sleeve surface, resulting in reduced e_m. The sleeve oscillates periodically as a pendulum due to the external harmonic load.

However, it will be shown that the complete dynamic behavior is more complex. The inertia and damping of the sleeve motion cause a phase lag between the sleeve and the force oscillations. In certain cases, depending on the design parameters, one can expect adverse effects. If the phase lag becomes excessive, it would result in unsynchronized sleeve rotation, opposite to the desired direction. This discussion emphasizes the significance of a full analysis, not only to predict behavior but also to provide the tools for proper design.

18.5.1 Equations of Motion

The following analysis is for a composite bearing operating at the rated constant journal speed, with the centrifugal restraint (Fig. 18-6). The length L of the internal bore of most rolling bearings is short relative to the diameter D. For this reason, the following is for a short journal bearing, which assumes $L \ll D$. The analysis can be extended to a finite-length journal bearing; however, it is adequate

for our purpose—to compare the dynamic behavior of a composite bearing to that of a regular one.

The first step is a derivation of the dynamic equation that describes the rotation of the composite bearing *sleeve unit*, consisting of the sleeve, the inner ring of the rolling bearing, and the centrifugal disc system. The three parts are tightly fitted and are rotating together at an angular speed ω_b, as shown in Fig. 18-8. This sleeve unit has an equivalent moment of inertia I_{eq}. The degree of freedom of sleeve rotation, which is involved with I_{eq}, includes the rolling elements that rotate at a reduced speed. It is similar to an equivalent moment of inertia of meshed gears.

A periodic load results in a variable hydrodynamic friction torque, and in turn there are angular oscillations of the sleeve unit (the angular velocity ω_b varies periodically). The sleeve unit oscillations are superimposed on a constant

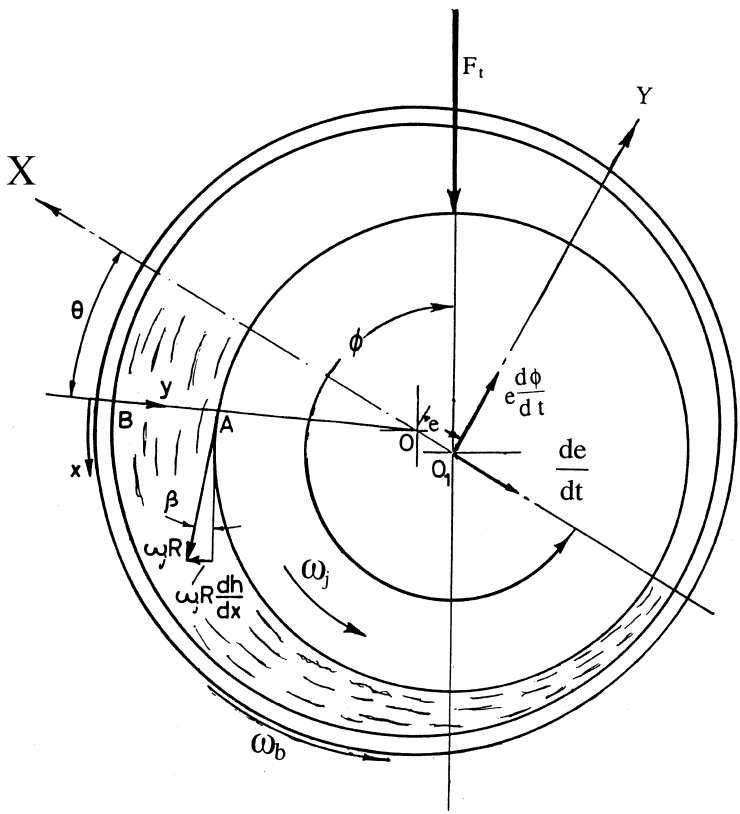

FIG. 18-8 Dynamically loaded composite bearing.

speed of rotation. At the same time, the mechanical friction between the pins and the housing damps these oscillations.

The difference between the hydrodynamic (viscous) friction torque M_h and the mechanical friction torque of the pins M_f is the resultant torque that accelerates the sleeve unit. The rolling friction torque M_r is small and negligible. The equation of the sleeve unit motion becomes

$$M_h - M_f = I_{\text{eq}} \frac{d\omega_b}{dt} \tag{18-12}$$

Substituting the values of the hydrodynamic torque and the mechanical friction torque from Eqs. (18-3) and (18-6) into Eq. (18-12) results in the following equation for the sleeve motion:

$$\frac{L\mu R^3}{C}(\omega_j - \omega_b)\frac{2\pi}{(1-\varepsilon^2)^{0.5}} - m_c R_m R_h \omega_b^2 f_c = I_{\text{eq}} \frac{d\omega_b}{dt} \tag{18-13}$$

This equation is converted to dimensionless form by dividing all the terms by $I_{\text{eq}}\omega_j^2$. The final dimensionless dynamic equation of the sleeve unit motion is

$$(1-\xi)H_1 \frac{2\pi}{(1-\varepsilon^2)^{0.5}} - \xi^2 H_2 = \dot{\xi} \tag{18-14}$$

Here, ξ is the ratio of the sleeve unit angular velocity to the journal angular velocity:

$$\xi = \frac{\omega_b}{\omega_j} \tag{18-15}$$

The time derivative $\dot{\xi} = d\xi/d\bar{t}$ is with respect to the dimensionless time, $\bar{t} = \omega_j t$, and the dimensionless parameters H_1 and H_2 are design parameters of the composite bearing defined by

$$H_1 = \frac{L\mu R^3}{C I_{\text{eq}} \omega_j}; \qquad H_2 = m_c R_m R_h f_c \tag{18-16}$$

18.5.2 Equation of Journal Motion

Chapter 7 presented the solution of Dubois and Ocvirk (1953) for the pressure distribution of a short journal bearing under steady conditions. This derivation was extended in Chapter 15 to a short bearing under dynamic conditions. In this chapter, this derivation is further extended to a composite bearing where the sleeve unit rotates at unsteady speed.

It was shown in Chapter 15 that in a journal bearing under dynamic conditions, the journal center O_1 has an arbitrary velocity described by its two

components, de/dt and $e\,d\phi/dt$, in the radial and tangential directions, respectively. The purpose of the following analysis is to solve for the journal center trajectory of a composite bearing.

Let us recall that the Reynolds equation for the pressure distribution p in a thin incompressible fluid film is

$$\frac{\partial}{\partial x}\left(\frac{h^3}{\mu}\frac{\partial p}{\partial x}\right)+\frac{\partial}{\partial z}\left(\frac{h^3}{\mu}\frac{\partial p}{\partial z}\right)=6(U_1-U_2)\frac{\partial h}{\partial x}+12(V_2-V_1) \tag{18-17}$$

Similar to the derivation in Sec. 15.2, the journal surface velocity components, U_2 and V_2 are obtained by summing the velocity vector of the surface velocity, relative to the journal center O_1 (velocity due to journal rotation), and the velocity vector of O_1 relative to O (velocity due to the motion of the journal center O_1). At the same time, the sleeve surface has only tangential velocity, $R\omega_b$, in the x direction. In a composite bearing, the fluid film boundary conditions on the right-hand side of Eq. (18-17) become

$$V_1=\omega_j R\frac{dh}{dt}+\frac{de}{dt}\cos\theta+e\frac{d\phi}{dt}\sin\theta \tag{18-18}$$

$$V_2=0 \tag{18-19}$$

$$U_1=\omega_b R \tag{18-20}$$

$$U_2=\omega_j R+\frac{de}{dt}\sin\theta-e\frac{d\phi}{dt}\cos\theta \tag{18-21}$$

According to our assumptions, $\partial p/\partial x$ on the left-hand side of Eq. (18-17) is negligible. Considering only the axial pressure gradient and substituting Eqs. (18-18)–(18-21) into Eq. (18-17) yields

$$\frac{\partial}{\partial z}\left(h^3\frac{\partial p}{\partial z}\right)=6\mu\frac{\partial}{\partial x}R(\omega_j+\omega_b)+6\mu\left(\frac{de}{dt}\cos\theta+e\frac{d\phi}{dt}\sin\theta\right) \tag{18-22}$$

Integrating Eq. (18-22) twice with the following boundary conditions solves the pressure wave:

$$p=0 \qquad \text{at} \quad z=\pm\frac{L}{2} \tag{18-23}$$

In the case of a short bearing, the pressure is a function of z and θ. The following are the two equations for the integration of the load capacity components in the directions of W_x and W_y:

$$W_x = -2R \int_0^{\pi} \int_0^{L/2} p \cos\theta \, d\theta \, dz \tag{18-24}$$

$$W_y = 2R \int_0^{\pi} \int_0^{L/2} p \sin\theta \, d\theta \, dz \tag{18-25}$$

The dimensionless load capacity W and the external dynamic load $F(t)$ are defined as follows:

$$\overline{W} = \frac{C^2}{\mu R \omega_j L^3} W; \qquad \overline{F}(t) = \frac{C^2}{\mu R \omega_j L^3} F(t) \tag{18-26}$$

where the journal speed ω_j is constant. After integration and conversion to dimensionless form, the following fluid film load capacity components are obtained:

$$\overline{W}_x = -\frac{1}{2} J_{12} \varepsilon (1 + \xi) + \varepsilon \dot{\phi} J_{12} + \dot{\varepsilon} J_{22} \tag{18-27}$$

$$\overline{W}_y = \frac{1}{2} J_{11} \varepsilon (1 + \xi) - \varepsilon \dot{\phi} J_{12} - \dot{\varepsilon} J_{22} \tag{18-28}$$

The integrals J_{ij} and their solutions are defined according to Eq. (7-13). The resultant of the load and fluid film force vectors accelerates the journal according to Newton's second law:

$$\vec{F}(t) + \vec{W} = m\vec{a} \tag{18-29}$$

Here, $\vec{a}$ is the acceleration vector of the journal center O_1 and m is the journal mass. Dimensionless mass is defined as

$$\overline{m} = \frac{C^3 \omega_j R}{L^3 R^2} m \tag{18-30}$$

After substitution of the acceleration terms in the radial and tangential directions (directions X and Y in Fig. 18-8) the equations become

$$\overline{F}_x(t) - \overline{W}_x = \overline{m}\ddot{\varepsilon} - \overline{m}\varepsilon\dot{\phi}^2 \tag{18-31}$$

$$\overline{F}_y(t) - \overline{W}_y = -\overline{m}\varepsilon\ddot{\phi} - 2\overline{m}\dot{\varepsilon}\dot{\phi} \tag{18-32}$$

Substituting the load capacity components of Eqs. (18-27) and (18-28) into Eqs. (18-31) and (18-32) yields the final two differential equations of the journal motion:

$$\overline{F}(t)\cos(\phi-\pi) = -0.5J_{12}\varepsilon(1+\xi) + \varepsilon\dot{\phi}J_{12} + \dot{\varepsilon}J_{22} + \overline{m}\ddot{\varepsilon} - \overline{m}\varepsilon\dot{\phi}^2 \tag{18-33}$$

$$\overline{F}(t)\sin(\phi-\pi) = 0.5J_{11}\varepsilon(1+\xi) - \varepsilon\dot{\phi}J_{11} - \dot{\varepsilon}J_{12} - \overline{m}\varepsilon\ddot{\phi} - 2\overline{m}\dot{\varepsilon}\dot{\phi} \tag{18-34}$$

Equations (18-33), (18-34), and (18-14) are the three differential equations required to solve for the three time-dependent functions ε, ϕ, and ξ. These three variables represent the motion of the shaft center O_1 with time, *in polar coordinates*, as well as the rotation of the sleeve unit.

18.5.3 Comparison of Journal Locus under Dynamic Load

In machinery there are always vibrations and bearing under steady loads are usually subjected to dynamic oscillating loads. The following is a solution for a composite bearing under a vertical load consisting of a sinusoidal load superimposed on a steady load according to the equation (in this section, $\bar{F}$ and $\bar{m}$ are renamed F and m)

$$F(t) = F_s + F_o \sin\alpha\omega_j t \tag{18-35}$$

Here, F_s is a steady load, F_o is the amplitude of a sinusoidal force, ω is the load frequency, and α is the ratio of the load frequency to the journal speed:

$$\alpha = \frac{\omega}{\omega_j} \tag{18-36}$$

Equations (18-33), (18-34), and (18-14) were solved by finite differences. By selecting backward differences, the nonlinear terms were linearized. In this way, the three differential equations were converted to three regular equations. The finite difference procedure is presented in Sec. 15.4.

Examples of the loci of a composite bearing and a regular journal bearing are shown in Fig. 18-9 for $\alpha = 2$ and in Fig. 18-10 for $\alpha = 2$ and $\alpha = 4$. Any reduction in the maximum eccentricity ratio, ε_m, represents a significant improvement in lubrication performance. The curves indicate that the composite bearing (dotted-line locus) has a lower ε_m than a regular journal bearing (solid-line locus). An important aspect is that the relative improvement increases whenever ε_m increases (the journal approaches the sleeve surface); thus, the composite bearing plays an important role in wear reduction. For example, in the heavily loaded

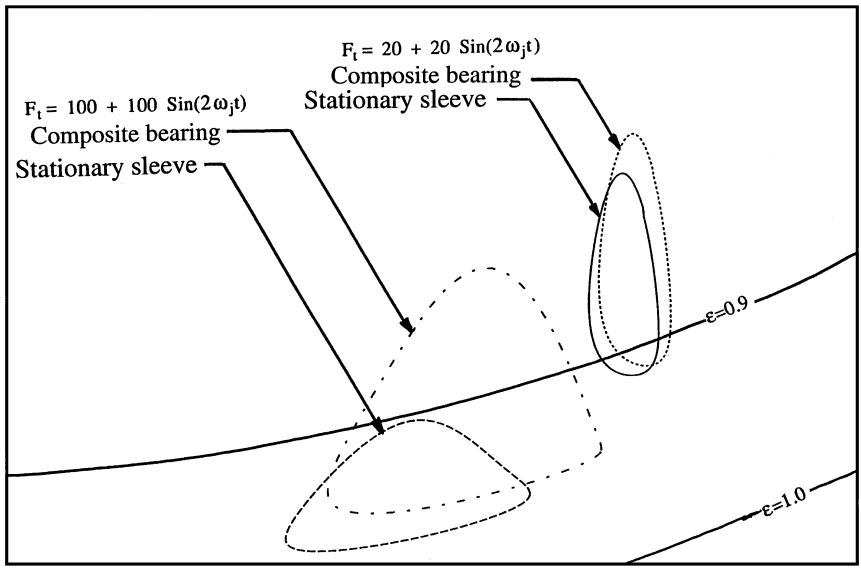

FIG. 18-9 Journal loci of a regular bearing and a composite bearing; $F(t) = 100 + 100\sin(2\omega_j t)$ and $F(t) = 20 + 20\sin(2\omega_j t)$. The journal mass is $m = 50$. The design parameters are $H_1 = 0.1$ and $H_2 = 1.0$.

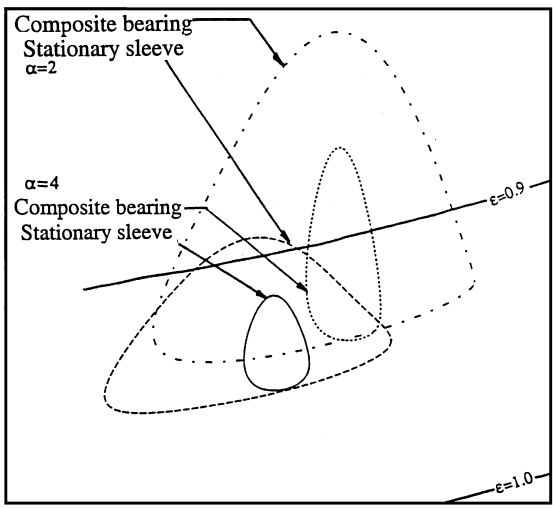

FIG. 18-10 Journal loci of rigid and compliant sleeve bearings. The load $F(t) = 100 + 100\sin(\alpha\omega_j t)$, for $\alpha = 2$ and $\alpha = 4$. The journal mass $m = 50$. $H_1 = 0.1$ and $H_2 = 1.0$.

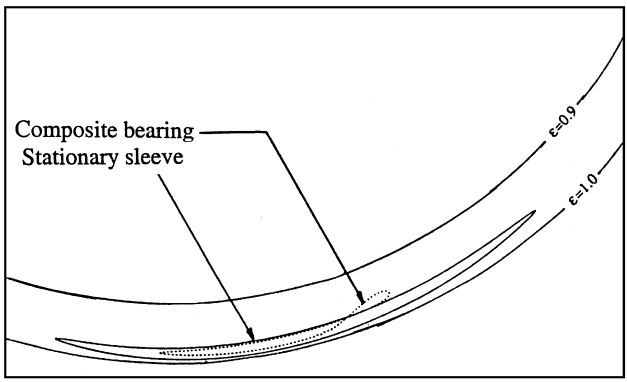

FIG. 18-11 Journal loci of rigid and compliant sleeve bearings under heavy load. $F(t) = 800 + 800\sin(2\omega_j t)$. The journal mass is $m = 100$, $H_1 = 0.1$ and $H_2 = 100$.

bearing in Fig 18-11, the composite bearing nearly doubles the minimum film thickness ε_m of a regular journal bearing. This can be observed by the distance between the two loci and the circle $\varepsilon = 1$.

If there is a relatively large phase lag between the load and sleeve unit oscillations, the lubrication performance of the composite bearing can deteriorate. In order to benefit from the advantages of a composite bearing, in view of the many design parameters, the designer must in each case conduct a similar computer simulation to determine the dynamic performance.

18.6 THERMAL EFFECTS

The peak temperature, in the fluid film and on the inner surface of the sleeve (near the minimum film thickness) was discussed in Sec. 8.6. Excessive peak temperature $T_{\max}$ can result in bearing failure, particularly in large bearings with white metal lining. Therefore, in these cases, it is necessary to limit $T_{\max}$ during the design stage.

With a properly designed composite bearing, a much more uniform temperature distribution is expected; since the sleeve unit rotates, the severity of the peak temperature is reduced.

The heat transfer from the region of the minimum film thickness to the atmosphere is affected by the rotation of the sleeve as well as many other parameters, such as bearing materials, lubrication, heat conduction at the contact between the rolling elements and races, the design of the bearing housing, and its connection to the body of the machine.

In order to elucidate the effect of the rotation of the sleeve on heat transfer, Harnoy and Khonsari (1996) studied the effect of sleeve rotation in isolation from

any other factor that can affect the rate of heat removal from the hydrodynamic oil film. For this purpose, the heat transfer problem of a hydrodynamic bearing at steady-state conditions is studied and a comparison made between the temperature distributions in stationary and rotary sleeves while all other parameters, such as geometry and materials, are identical for the two cases. For comparison purposes, a model is presented where the sleeve loses heat to the surroundings at ambient temperature T_{amb}. It has been shown that such a model can yield practical conclusions concerning the thermal effect of the rotating sleeve in the composite bearing.

An example of a typical hydrodynamic bearing is selected. The purpose of the analysis is to determine the temperature distributions inside the rotating and stationary sleeves. The geometrical parameters and operating conditions of the two hydrodynamic bearings are summarized in Table 18.1.

18.6.1 Thermal Solution for Stationary and Rotating Sleeves

The temperature distribution in the fluid film is solved by the Reynolds equation, together with the equation of viscosity variation versus temperature. The viscous friction losses are dissipated in the fluid as heat, which is transferred by convection (fluid flow) and conduction through the sleeve. The shaft temperature

TABLE 18-1 Bearing and Lubrication Specifications

Outer sleeve radius, R_o	0.095 m
Shaft radius, R_j	0.05 m
Shaft speed, ω_j	3500 RPM
Sleeve wall thickness, b	0.01 m
Sleeve length, L	0.1 m
Sleeve thermal diffusivity, α_b	$1.5 \times 10^{-5} m^2/s$
Sleeve speed, ω_b	200 RPM
Clearance, C	0.00006 m
Eccentricity ratio, ε	0.5
Length-to-diameter ratio, L/D	1
Thermal conductivity of sleeve material, K_b	45 W/m-K
Density of bush material, ρ_b	$8666\ kg/m^3$
Specific heat of sleeve material, C_{pb}	0.343 kJ/kg-K
Thermal conductivity of oil, K_o	0.13 W/m-K
Density of oil, ρ_o	$860\ kg/m^3$
Ambient temperature, T_{amb}	24.4°C
Viscosity of the oil at the inlet temperature, μ	0.03 kg/m-s
Viscosity–temperature coefficient, β	0.0411/°K
Oil thermal diffusivity, α_o	$7.6 \times 10^8\ m^2/s$

From Harnoy and Khonsari, 1996.

is assumed to be constant. The following equation, in a cylindrical coordinate system (r, θ), was used for solving the temperature distribution in the sleeve (the coordinate system is fixed to the solid sleeve and rotating with it):

$$\frac{\partial^2 T}{\partial r^2} + \frac{1}{r}\frac{\partial T}{\partial r} + \frac{1}{r^2}\frac{\partial^2 T}{\partial \theta^2} = \frac{1}{\alpha}\frac{dT}{dt} \tag{18-37}$$

where α is the thermal diffusivity of the solid. For a rotating sleeve in stationary (Eulerian) coordinates (the sleeve rotates relative to the stationary coordinates) this equation can be expressed as

$$\frac{\partial^2 T}{\partial r^2} + \frac{1}{r}\frac{\partial T}{\partial r} + \frac{1}{r^2}\frac{\partial^2 T}{\partial \theta^2} = \frac{\omega_b}{\alpha}\frac{\partial T}{\partial \theta} + \frac{1}{\alpha}\frac{dT}{dt} \tag{18-38}$$

where ω_b is the angular speed of the sleeve.

The following order of magnitude analysis intends to show that when the sleeve rotates above a certain speed, its maximum temperature difference in the circumferential direction, ΔT_c, becomes negligible compared with the maximum temperature difference, ΔT_r, in the radial direction. The order of magnitude of all terms in Eq. (18-38) are:

$$\begin{aligned} \frac{\partial^2 T}{\partial r^2} &= O\left(\frac{\Delta T_r}{b^2}\right) \\ \frac{1}{r}\frac{\partial T}{\partial r} &= O\left(\frac{\Delta T_r}{R_b b}\right) \\ \frac{1}{r^2}\frac{\partial^2 T}{\partial \theta^2} &= O\left(\frac{\Delta T_c}{\pi R_b^2}\right) \end{aligned} \tag{18-39a}$$

$$\frac{\omega_b}{\alpha}\frac{\partial T}{\partial \theta} = O\left(\frac{\omega_b R_b}{\alpha}\right)\left(\frac{\Delta T_c}{R_b}\right) \tag{18-39b}$$

Here, b represents the sleeve wall thickness, $b = R_o - R_i$. The radius R is taken as the average value of the outer and inner radii of the bushing, $R_b = (R_o + R_i)/2$. Substituting these orders in Eq. (18-38) and assuming $b \ll R$, the order of the ratio of the temperature gradients is

$$\frac{\dfrac{\partial T}{\partial r}}{\dfrac{1}{R}\dfrac{\partial T}{\partial \theta}} = O\left(\frac{\omega_b R_b b}{\alpha_b}\right) \tag{18-40}$$

The dimensionless parameter on the right-hand side of Eq. (18-40) is a modified Peclet number (Pe). Equation (18-40) indicates that when $\mathrm{Pe} \gg 1$, the radial temperature gradient is much higher than the temperature gradient in the circumferential direction, and the temperature distribution can be assumed to

be uniform around the sleeve. In fact, in the circumferential direction, most of the heat is effectively transferred by the moving mass of the rotating sleeve and only a negligible amount of heat is transferred by conduction. In the example (Table 18-1), if the sleeve speed is 200 RPM, the Peclet number is

$$\mathrm{Pe} = \frac{\omega_b R_b b}{\alpha_b} = 692 \tag{18-41}$$

This number indicates that the circumferential temperature gradient is relatively low, and only heat conduction in the radial direction needs to be considered in solving for the temperature distribution. It is interesting to note that there would be no significant change in the composite bearing thermal characteristics even at much lower sleeve speeds. For example, for $\omega_b = 30$ RPM, the resulting Pe is above 100, and the assumption of negligible circumferential temperature gradients should still hold. It should be noted that a composite bearing design operating at a low sleeve speed might not be desirable. Elastohydrodynamic lubrication in the rolling bearing requires a certain minimum speed below which

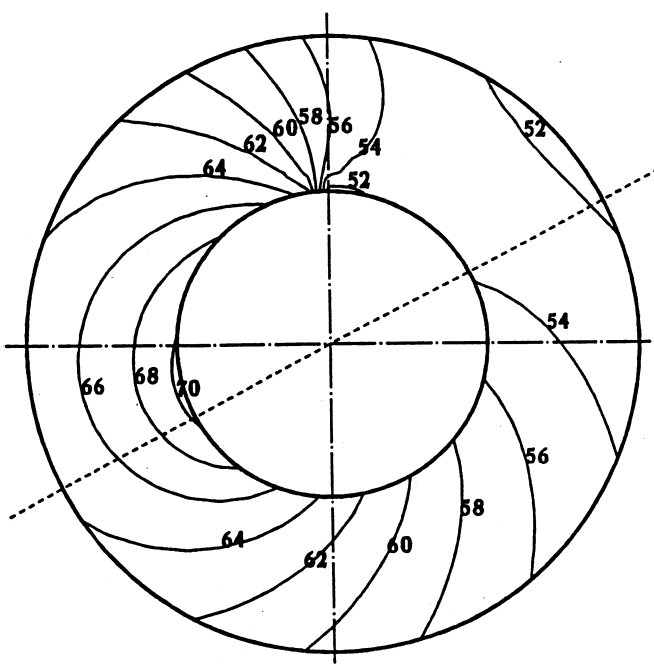

FIG. 18-12 Thermohydrodynamic solution showing the isotherm contours plot in a stationary sleeve of a journal bearing. $L/D = 1$, $\varepsilon = 0.5$, $N_{\text{shaft}} = 3500$ RPM. (From Harnoy and Khonsari, 1996.)

the friction is somewhat higher, as the rolling bearing friction–velocity curve presented in Fig. 18-4 demonstrates.

A full thermohydrodynamic analysis was performed with the bearing specifications listed in Table 18-1 assuming a stationary sleeve. The solution for the temperature profile in the stationary sleeve is presented by isotherms in Fig. 18-12.

Hydrodynamic lubrication theory indicates that the amount of heat dissipated in the oil film is proportional to the average shear rate and, in turn, proportional to the difference between the journal and sleeve speeds $(\omega_j - \omega_b)$. Therefore, it is reasonable to assume that the heat flux from the oil film to the surroundings is also proportional to $(\omega_j - \omega_b)$. Therefore, the ratio of the radial heat fluxes of rotating and stationary is

$$Q_{\text{rotating sleeve}} = Q_{\text{rigid sleeve}} \frac{(\omega_j - \omega_b)}{\omega_j} \tag{18-42}$$

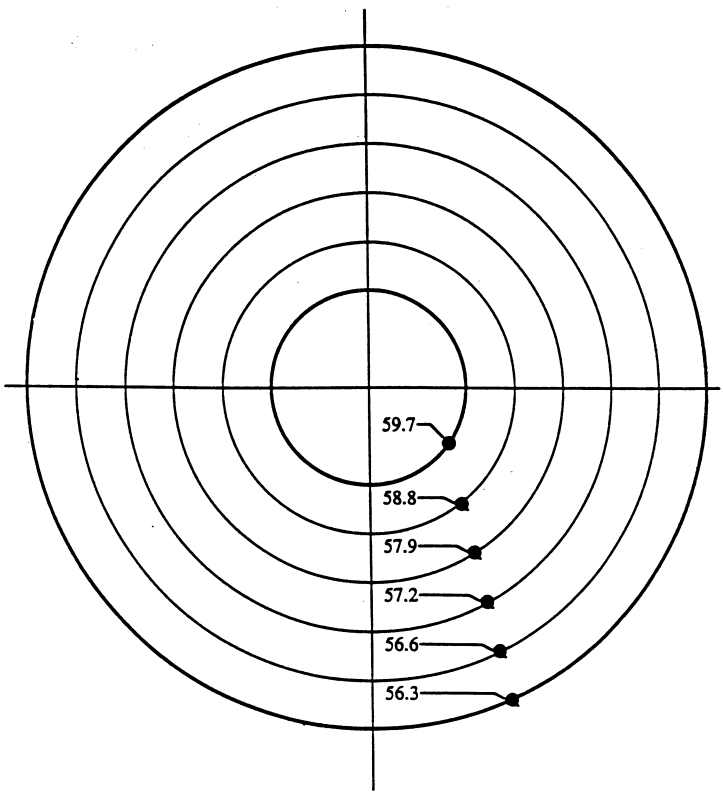

FIG. 18-13 Isotherm contours plot of a rotating sleeve unit. (From Harnoy and Khonsari, 1996.)

The surface temperatures T_i (inner wall) and T_o (outside wall) of the sleeve are solved by the following equations:

$$T_i = T_{\text{amb}} + Q_{\text{rotating sleeve}} \left\{ \frac{\ln(R_o/R_i)}{2\pi k_b L} + \frac{1}{2\pi R_o L h} \right\} \tag{18-43}$$

$$T_o = T_i - Q_{\text{rotating sleeve}} \left\{ \frac{\ln(R_o/R_i)}{2\pi k_b L} \right\} \tag{18-44}$$

Here, h is the correction coefficient. The temperature distribution in the sleeve is obtained from

$$\frac{T - T_i}{T_o - T_i} = \frac{\ln(r/R_i)}{\ln(R_o/R_i)} \tag{18.45}$$

The results are circular isotherms, as shown in Fig. 18-13. The uniformity in the temperature profile, together with a reduction in the maximum temperature (59.7°C for composite bearing versus 71°C for a conventional hydrodynamic bearing), is indicative of the superior thermal performance.